Research Article

Andrey N. Chibisov*, Maxim A. Pugachevskii, Alexander P. Kuzmenko, Myo Min Than, and Alexey I. Kartsev

Effect of morphology and size on the thermodynamic stability of cerium oxide nanoparticles: Experiment and molecular dynamics calculation

https://doi.org/10.1515/ntrev-2022-0038
received October 21, 2021; accepted January 1, 2022

Abstract: Cerium oxide nanoparticles have unique catalytic and oxygen storage capacity properties. In this work, the morphology and size of cerium oxide nanoparticles were experimentally and theoretically investigated. For the synthesis of nanoparticles, the laser ablation method was used. The analysis of the size and morphological characteristics of nanoparticles was performed using transmission electron microscopy. Using the method of molecular dynamics, we reveal the limiting dimensional transition from octahedral morphology to a spherical form in cerium oxide nanoparticles. The results obtained will be relevant for the controlled synthesis of nanostructured materials based on cerium oxide.

Keywords: nanoparticles, cerium oxide, size and morphology, TEM microscopy, molecular dynamics

1 Introduction

Due to its unique properties, nanostructured cerium oxide is commonly used in solid oxide fuel cells [1] and as a catalyst [2]. Understanding its main properties such as high oxygen storage capacity, redox catalytic properties [3], and electronic properties is an important step to creating highly promising nanomaterials based on cerium oxide nanoparticles. For a detailed understanding of these processes, it is necessary to consider the dimensional, morphological, and thermodynamic features of nanostructured compounds based on CeO_2. Recent experimental studies show that the lattice parameters increase with a decrease in the size of cerium oxide nanoparticles. The authors explain this lattice expansion as a result of the formation of significant amounts of Ce^{3+} with corresponding oxygen vacancies [4–6]. Our theoretical calculations within the framework of the density functional theory confirm this result [7]. In refs. [8,9], it was shown that the surface energies of cerium oxide are characterized by the relationship (111) < (110) < (100). These surfaces, depending on the size of the CeO_2 nanoparticles, determine their morphology according to the Wulff rule [10,11]. The synthesis of the nanocrystalline cerium oxide uses various common physicochemical methods such as the co-precipitation method [3], the solvothermal method [12,13], the hydrothermal method [11], pyrolysis [14], the sol–gel process [15], *etc*. These methods can produce cubic, octahedral, spherical, and other forms of CeO_2 nanoparticles. In particles with a more developed morphology, the physicochemical activity increases significantly. So, for cubic and octahedral particles in comparison with spherical particles of the same volume, the specific surface area increases significantly. In addition, at the boundaries and vertices of the faces, favorable conditions arise for the formation of structural defects, which contribute to a significant increase in the catalytic, nanoelectronic, energy storage, and biomedical properties of particles.

One of the most promising methods for nanostructuring a substance, especially for obtaining nanoparticles, is laser ablation [16,17]. The advantage of this method is the possibility of obtaining metastable condensed phases due to the development of high-temperature gradients in the process of ultrafast heating and cooling of matter.

* **Corresponding author: Andrey N. Chibisov,** Computing Center of FEB RAS, 65 Kim Yu Chen St., Khabarovsk, 680000, Russia, e-mail: andreichibisov@yandex.ru
Maxim A. Pugachevskii, Alexander P. Kuzmenko, Myo Min Than: Southwest State University, 94, 50 Let Oktyabrya St., Kursk, 305040, Russia
Alexey I. Kartsev: Computing Center of FEB RAS, 65 Kim Yu Chen St., Khabarovsk, 680000, Russia; Bauman Moscow State Technical University, Moscow, 105005, Russia

These physical processes are characterized by the accumulation of structural defects in the nanoparticles' crystal structure that can affect the functional properties of CeO_2 when it is used in applied problems, such as photocatalysis [18], thermoelastic stabilization [19], and antioxidant properties [20]. When cerium oxide nanoparticles are obtained using laser ablation [21,22], there is a strong scatter in the particle sizes, and, in general, they are characterized by octahedral and spherical morphology [23,24]. However, at what nanoparticles diameter and why the transition from octahedral to spherical morphology occurs is still unclear. For a more detailed and accurate description of the properties of nanosized systems based on cerium oxide nanoparticles, it is necessary to use computational methods capable of describing the structure and morphology of the nanoparticles for sufficiently large sizes. The molecular dynamics method served such a computational technology.

This work is devoted to the experimental and theoretical study of the morphology of cerium oxide nanoparticles. Here, the cerium oxide nanoparticles were produced by laser ablation; the analysis of the size and morphological characteristics of the nanoparticles was carried out using transmission electron microscopy. Using the method of molecular dynamics, the agglomeration of CeO_2 nanoparticles depending on their size has been calculated for the first time. With the help of our studies, we were able to identify the phase transition from octahedral to spherical morphology and determined the limiting size of this transition.

2 Experiments and calculations

2.1 Materials and methods

Cerium dioxide nanoparticles were obtained by pulsed sputtering of the target material using an IPG Photonics diode-pumped ytterbium fibre laser with the HighContrast option (radiation wavelength: 1.06 μm, laser radiation intensity: 10^{10} W m^{-2}, pulse duration: 200 μs, and pulse repetition rate: up to 1 kHz). The target for laser ablation was a tablet of remelted chemically pure (>99.99%) cerium dioxide powder. Under the action of focused laser radiation, cerium dioxide was explosively sprayed, forming a flow of ablated particles [18,19,25]. Layers of ablated cerium dioxide nanoparticles were deposited onto a silicon wafer. The spraying time was 1–10 min. Then, the resulting particles were dispersed in an ultrasonic bath for at least 40 min. Deionized water was used as a solvent. After dispersion, the nanodispersed solution of cerium dioxide was centrifuged at various spin rates in the range from 800 to 13,400 rpm to minimize the limiting particle size. After centrifugation of the colloidal CeO_2 system at 500 rpm, the limiting particle size in the colloidal system is reduced up to 80 nm; at 2,000 rpm, 50 nm; at 5,000 rpm, 40 nm; and, at 12,500 rpm, 30 nm [26]. Cerium dioxide nanoparticles were characterized using transmission electron microscopy (ZEISS LIBRA-120). For size and morphological analysis, several TEM images (more than 10 images for each sample) were used and the data are subsequently summarized.

2.2 Calculation methods

To carry out molecular dynamics calculations for cerium oxide nanoparticles, we used the Desmond package [27] implemented on the basis of "neutral territory" methods with a high degree of computational parallelism [28–30]. This software package has previously been successfully used to simulate the behaviour of CeO_2 nanoparticles [31]. All calculations were carried out at a constant temperature of 300 K and pressure of 1 bar within the *NPT* ensemble (a statistical mechanical ensemble that maintains constant temperature T, constant pressure P, and a constant number of particles N). For electrostatic and van der Waals interactions, we used a cut off at 9 Å taking into account the reversible reference system propagator algorithms (RESPA integrator) [32]. To describe the boundary conditions, all particles were placed in a cell with an orthorhombic shape.

3 Results and discussions

The TEM images of cerium oxide nanoparticles obtained by laser ablation are shown in Figure 1a. The results show

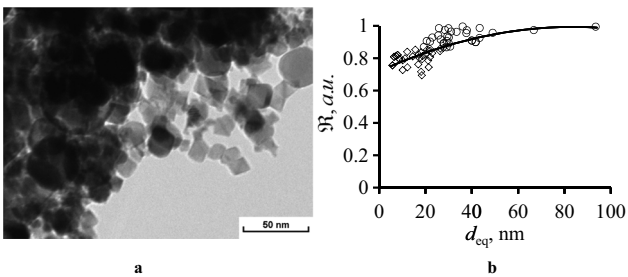

Figure 1: (a) Transmission electron microscopy image of cerium oxide nanoparticles obtained by laser ablation. (b) Dependence of the degree of nanoparticles' sphericity on their size.

that ablated nanoparticles have a wide size variation from 5 to 200 nm and can be characterized by both octahedral and spherical morphology. To determine the sphericity degree of the nanoparticles, the characteristic parameter of the sphericity coefficient was chosen:

$$\Re = \sqrt{\frac{d}{D}}, \quad (1)$$

where d and D are the diameters of the inscribed and described spheres for a nanoparticle of a certain size. The results of the analysis of TEM images show (Figure 1b) that an octahedral morphology is observed for ablated nanoparticles with sizes less than 23 nm, and a more spherical shape of particles is characteristic for sizes larger than 23 nm (the particle size was characterized by an equivalent spherical diameter for a sphere that has a volume equal to the volume of the particle). To explain this effect, the method of molecular dynamics was used.

According to transmission electron microscopy, X-ray diffractometry, and electron energy loss spectroscopy studies, it has recently been established that the ablated CeO_2 nanoparticles are enriched in oxygen vacancies that stabilize their internal structure. At this, with a decrease in the particle size, the concentration of crystal defects in the ablated particles increases [20]. The methodology of the laser ablation experiment is such that nanoparticles are sprayed in air under the influence of high temperature, and when they are deposited on a substrate (in our experiment on silicon), they quickly cool to room temperature. Therefore, molecular dynamics were simulated at a temperature of 300 K. The purpose of the calculations using molecular dynamics was to reveal the regularities of the agglomeration of CeO_2 nanoparticles during their synthesis by laser ablation.

We began our calculations of molecular dynamics by studying the interaction of three nanoparticles with a composition $Ce_{231}O_{448}$. We studied this nanoparticle size using the electron density functional theory method in our previous work [7]. Unfortunately, these are the largest cerium oxide nanoparticles that we could calculate within the DFT method using the Vasp software package [33,34] and the computational resources at our disposal. Therefore, it is logical that we took the particle data as the objects of the computational experiment. Initially, the particles were positioned randomly with respect to each other. Then, after a specified simulation time of 8,000 ps, three nanoparticles agglomerate into the structure shown in Figure 2a. They form a particle with a size of about 4.7 nm. Moreover, it can be seen that it is more advantageous for the particles to combine with each other, mainly *via* the (111) faces. The results are in good agreement with the theoretical data of ref. [35], carried out by the density functional theory method. When nine nanoparticles of cerium oxide are combined (Figure 2b), they tend to form an octahedral nanoparticle with a size of 7.3 nm. The total number of atoms in this nanoparticle is 6,111, of which 2,079 are Ce and 4,032 are O atoms. When 27 nanoparticles are combined, the same pattern is observed: the particles agglomerate and try to form an octahedron with an average size of 10 nm (Figure 3a). This particle contains 6,237 Ce and 12,096 O atoms. A further increase in the number of combined nanoparticles leads to an increase in the size of the total agglomerated particle, and a spherical morphology is observed to form beyond 20.6 nm. Thus, our calculations show that with an increase

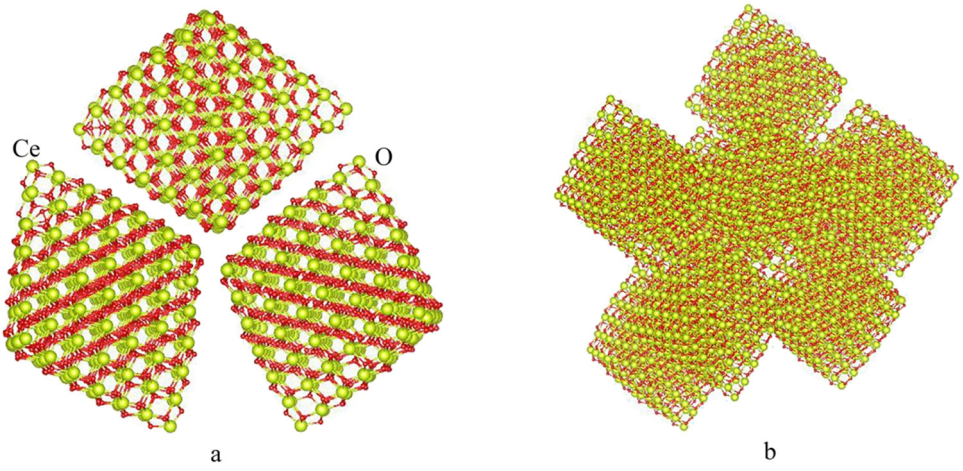

Figure 2: Structure of agglomerated nanoparticles with a size of (a) 4.7 nm and (b) 7.3 nm. The cerium and oxygen atoms are depicted by yellow and red balls, respectively.

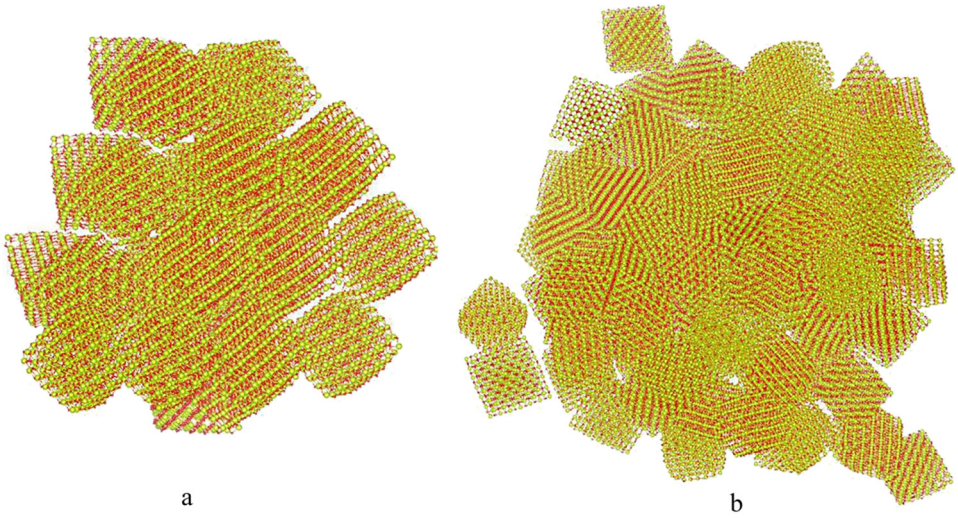

Figure 3: Structure of agglomerated octahedral and spherical nanoparticles: (a) 10 nm in size and (b) 20.6 nm in size.

in the size of cerium oxide nanoparticles over 20 nm, spherical nanoparticles become more stable than the octahedral forms. The calculations are in good agreement with the experimental data acquired in this work, where the experimental value of the transition size from octahedral to spherical morphology was 23 nm.

4 Conclusion

In this work, experimental and theoretical studies of the influence of morphological and dimensional parameters on the thermodynamic stability of cerium oxide nanoparticles were carried out. The cerium oxide nanoparticles were synthesized using the laser ablation method, and the size and morphological characteristics of nanoparticles were analysed using transmission electron microscopy. Experimental data have shown that the resulting nanoparticles predominantly have octahedral and spherical morphology with a particle size ranging from 5 to 200 nm. Using the molecular dynamics method, we have shown that with an increase in the size of cerium oxide nanoparticles to more than 20 nm, spherical nanoparticles become more stable than the octahedral forms. This result is in good agreement with our experimental data of the transition size from an octahedral morphology to a spherical one equal to 23 nm. Our novel results will be important for the analysis and planning of controlled synthesis of high-quality nanomaterials based on cerium oxide nanoparticles with the aim of their promising application in catalysis, nanoelectronics, and biomedicine.

Funding information: This study was carried out with the financial support of the Russian Foundation for Basic Research within the framework of scientific project no. 20-02-00599, as well as with the support of the Ministry of Education and Science of the Russian Federation, s/o 2020 no. 0851-2020-0035, prioritet-2030 program. The studies were carried out using the resources of the Center for Shared Use of Scientific Equipment and the Center for Processing and Storage of Scientific Data of the Far Eastern Branch of the Russian Academy of Sciences, funded by the Russian Federation represented by the Ministry of Science and Higher Education of the Russian Federation under project No. 075-15-2021-663. The authors would like to thank them for providing access to the HPC cluster atthe Joint Supercomputer Center of the Russian Academy of Sciences (JSCC RAS).

Author contributions: All authors have accepted responsibility for the entire content of this manuscript and approved its submission.

Conflict of interest: The authors state no conflict of interest.

References

[1] Wang B, Zhu B, Yun S, Zhang W, Xia C, Afzal M, et al. Fast ionic conduction in semiconductor $CeO_{2-\delta}$ electrolyte fuel cells. NPG Asia Mater. 2019;11:51.

[2] Montini T, Melchionna M, Monai M, Fornasiero P. Fundamentals and catalytic applications of CeO_2-based materials. Chem Rev. 2016;116:5987.

[3] Trovarelli A. Catalysis by ceria and related materials. London: Imperial College Press; 2002.
[4] Wu L, Wiesmann HJ, Moodenbaugh AR, Klie RF, Zhu Y, Welch DO, et al. Oxidation state and lattice expansion of CeO_{2-x} nanoparticles as a function of particle size. Phys Rev B. 2004;69:125415.
[5] Hailstone RK, DiFrancesco AG, Leong JG, Allston TD, Reed KJ. A study of lattice expansion in CeO_2 nanoparticles by transmission electron microscopy. J Phys Chem C. 2009;113:15155–9.
[6] Paun C, Safonova OV, Szlachetko J, Abdala PM, Nachtegaal M, Sa J, et al. Polyhedral CeO_2 nanoparticles: size-dependent geometrical and electronic structure. J Phys Chem C. 2012;116:7312–7.
[7] Pugachevskii MA, Chibisov AN, Kuzmenko AP, Fedorov AS. Theoretical and experimental studies of structural defects in CeO_2 nanoparticles. Solid State Phenom. 2020;312:68–73.
[8] Skorodumova NV, Baudin M, Hermansson K. Surface properties of CeO_2 from first principles. Phys Rev B. 2004;69:075401.
[9] Branda MM, Ferullo RM, Causa M, Illas F. Relative stabilities of low index and stepped CeO_2 surfaces from hybrid and GGA + U implementations of density functional theory. J Phys Chem C. 2011;115:3716–21.
[10] Cerf R. The Wulff crystal in Ising and percolation models. Berlin: Springer; 2006.
[11] Wang ZL, Feng X. Polyhedral shapes of CeO_2 nanoparticles. J Phys Chem B. 2003;107(49):13563–6.
[12] Fu C, Li R, Zhang Y. Synthesis and crystallization of nano-ceria particles by solvothermal routes. Int J Mod Phys B. 2010;24(15–16):3230–5.
[13] Florea I, Feral-Martin C, Majimel J, Ihiawakrim D, Hirlimann C, Ersen O. Three-dimensional tomographic analyses of CeO_2 nanoparticles. Cryst Growth Des. 2013;13:1110–21.
[14] Xu H, Gao L, Gu H, Guo J, Yan D. Synthesis of solid, spherical CeO_2 particles prepared by the spray hydrolysis reaction method. J Am Ceram Soc. 2002;85(1):139–44.
[15] Verma A, Karar N, Bakhshi AK, Chander H, Shivaprasad SM, Agnihotry SA. Structural, morphological and photoluminescence characteristics of sol–gel derived nano phase CeO_2 films deposited using citric acid. J Nanopart Res. 2007;9:317–22.
[16] Stafe M, Marcu A, Puscas NN. Pulsed laser ablation of solids: basics, theory and applications. Berlin: Springer-Verlag; 2014.
[17] Mihailescu IN, Caricato AP. Pulsed laser ablation advances and applications in nanoparticles and nanostructuring thin films. Singapore: Pan Stanford Publishing Pte. Ltd; 2018.
[18] Pugachevskii MA. Formation of TiO_2 nanoparticles by laser ablation and their properties. Nanosci Nanotechnol Lett. 2014;6:519–23.
[19] Pugachevskii MA. Stabilization of the high temperature phases of HfO_2 by pulsed laser irradiation. Inorg Mater. 2014;50(6):582–5.
[20] Pugachevskii MA, Chibisov AN, Mamontov VA, Kuzmenko AP. Antioxidant properties of stabilized CeO_2 nanoparticles. Phys Status Solidi A. 2021;1–5:2100355.
[21] Pugachevskii MA. Structural-defect formation in CeO2 nanoparticles upon laser ablation. Tech Phys Lett. 2017;43(8):698–700.
[22] Trenque I, Magnano GC, Bárta J, Chaput F, Bolzinger MA, Pitault I, et al. Synthesis routes of CeO_2 nanoparticles dedicated to organophosphorus degradation: a benchmark. Cryst Eng Comm. 2020;22:1725–37.
[23] Svetlichnyi VA, Lapin IN. Production of CeO_2 nanoparticles by method of laser ablation of bulk metallic cerium targets in liquid. Russ Phys J. 2016;58(11):1598–604.
[24] Takeda Y, Mafuné F. Formation of wide bandgap cerium oxide nanoparticles by laser ablation in aqueous solution. Chem Phys Lett. 2014;599:110–5.
[25] Pugachevskii MA, Zavodinskii VG, Kuz'menko AP. Dispersion of zirconium dioxide by pulsed laser radiation. Tech Phys. 2011;56(2):254–8.
[26] Pugachevskii MA, Mamontov VA, Aung NV, Chekadanov AS, Kuz'menko AP. Production of ablated CeO_2 particles with nanodispersed compositional distribution. Tech Phys Lett. 2020;46(10):1032–5.
[27] Bowers KJ, Chow E, Xu H, Dror RO, Eastwood MP, Gregersen BA, et al. Scalable algorithms for molecular dynamics simulations on commodity clusters. Proceedings of the ACM/IEEE Conference on Supercomputing (SC2006). New York: ACM Press; 2006. p. 2006.
[28] Shaw DE. A fast, scalable method for the parallel evaluation of distance-limited pairwise particle interactions. J Comput Chem. 2005;26:1318–28.
[29] Bowers KJ, Dror RO, Shaw DE. The midpoint method for parallelization of particle simulations. J Chem Phys. 2006;124:184109.
[30] Bowers KJ, Dror RO, Shaw DE. Zonal methods for the parallel execution of range limited N-body simulations. J Comput Phys. 2007;221:303–29.
[31] Kaushik AC, Bharadwaj S, Kumar S, Wei D-Q. Nano-particle mediated inhibition of Parkinson's disease using computational biology approach. Sci Rep. 2018;8:9169.
[32] Tuckermanan M, Berne BJ, Martyna GJ. Reversible multiple time scale molecular dynamics. J Chem Phys. 1992;97(3):1990.
[33] Kresse G, Joubert D. From ultrasoft pseudopotentials to the projector augmented-wave method. Phys Rev B. 1999;59:1758–75.
[34] Dudarev SL, Botton GA, Savrasov SY, Humphreys CJ, Sutton AP. Electron-energy-loss spectra and the structural stability of nickel oxide: an LSDA + U study. Phys Rev B. 1998;57:1505.
[35] Kim B-H, Kullgren J, Wolf MJ, Hermansson KH, Broqvist P. Multiscale modeling of agglomerated ceria nanoparticles: interface stability and oxygen vacancy formation. Front Chem. 2019;7:203.